Electronic Supplementary Material (ESI) for ChemComm.

Open-shell extensions to closed-shell pCCD

Katharina Boguslawski[a]

[a] *Institute of Physics, Faculty of Physics, Astronomy and Informatics, Nicolaus Copernicus University in Toruń, Grudziadzka 5, 87-100 Torun, Poland; E-mail: k.boguslawski@fizyka.umk.pl*

Electronic Supplementary Information

S1 A brief introduction to the equation of motion formalism

In order to model excited states in CC theory, the equation of motion (EOM) formalism[15–17] can be applied. EOM-CC[17–20] uses a linear ansatz to parametrize the k-th state

$$|\Psi_k\rangle = \hat{R}(k)\,|\mathrm{CC}\rangle\,, \tag{1}$$

where the operator $\hat{R}(k)$ generates the targeted state k from the initial CC reference state,

$$|\Psi_0\rangle = e^{\hat{T}}\,|\Phi_0\rangle\,. \tag{2}$$

In this work, the cluster operator $\hat{T}$ is restricted to electron pair excitations of pCCD, $\hat{T} = \hat{T}^{\mathrm{pCCD}}$. All equations below are, however, expressed in their general form exploiting some CC reference state. The explicit form of the operator $\hat{R}(k)$ determines the EOM flavor, like electron excitation, ionization, electron attachment, or spin flip.

Specifically for electronically excited (EE) states, the operator $\hat{R}(k)$ is particle- and spin-conserving and contains 1 hole (h) and 1 particle (p) operators, 2h2p operators, etc.,

$$\hat{R}^{\mathrm{EE}}(k) = \sum_{ia} r_i^a(k)\hat{a}^\dagger\hat{i} + \frac{1}{4}\sum_{ijab} r_{ij}^{ab}(k)\hat{a}^\dagger\hat{b}^\dagger\hat{j}\hat{i} + \ldots = \hat{R}_{1\mathrm{h}1\mathrm{p}}(k) + \hat{R}_{2\mathrm{h}2\mathrm{p}}(k) + \ldots$$

In the ionization potential (IP) EOM-CC formalism, the operator $\hat{R}(k)$ is composed of 1h operators, 2h1p operators, etc.,

$$\hat{R}^{\mathrm{IP}}(k) = \sum_{i} r_i(k)\hat{i} + \frac{1}{2}\sum_{ija} r_{ij}{}^{a}(k)\hat{a}^\dagger\hat{j}\hat{i} + \ldots = \hat{R}_{1\mathrm{h}}(k) + \hat{R}_{2\mathrm{h}1\mathrm{p}}(k) + \ldots$$

Thus, the single ionization problem annihilates electrons in the (occupied) levels i and may perform electron excitations from occupied to virtual spin orbitals. In the double (D)IP-EOM flavor, the operator $\hat{R}(k)$ contains 2h operators, 3h1p operators, etc.,

$$\hat{R}^{\mathrm{DIP}}(k) = \frac{1}{2}\sum_{i} r_{ij}(k)\hat{j}\hat{i} + \frac{1}{6}\sum_{ijka} r_{ijk}{}^{a}(k)\hat{a}^\dagger\hat{k}\hat{j}\hat{i} + \ldots = \hat{R}_{2\mathrm{h}}(k) + \hat{R}_{3\mathrm{h}1\mathrm{p}}(k) + \ldots$$

In the double ionization problem, we thus annihilate two electrons in the occupied spin orbitals i, j.

In the electron attachment variant of EOM-CC, the role of particle and hole operators (or lines in the corresponding diagrams, respectively) is reversed. Specifically, in electron affinity (EA) EOM-CC, the operator $\hat{R}(k)$ contains 1p operators, 1h2p operators, etc.,

$$\hat{R}^{\mathrm{EA}}(k) = \sum_{a} r^a(k)\hat{a}^\dagger + \frac{1}{2}\sum_{abi} r_i^{ab}(k)\hat{a}^\dagger\hat{b}^\dagger\hat{i} + \ldots = \hat{R}_{1\mathrm{p}}(k) + \hat{R}_{1\mathrm{h}2\mathrm{p}}(k) + \ldots,$$

while the double (D)EA-EOM-CC ansatz includes 2p operators, 1h3p operators, etc.,

$$\hat{R}^{\mathrm{DEA}}(k) = \frac{1}{2}\sum_{ab} r^{ab}(k)\hat{a}^\dagger\hat{b}^\dagger + \frac{1}{6}\sum_{abci} r_i^{abc}(k)\hat{a}^\dagger\hat{b}^\dagger\hat{c}^\dagger\hat{i} + \ldots = \hat{R}_{2\mathrm{p}}(k) + \hat{R}_{1\mathrm{h}3\mathrm{p}}(k) + \ldots$$

While the standard formulations of the IP and EA flavors of EOM-CC exploit a closed-shell reference, the spin-flip[18,21] (SF) variant uses a high-spin reference and spin-flipping $\hat{R}(k)$ operators, that is, excitation operators that include a spin-flip of one electron ($\alpha \rightarrow \beta$),

$$\hat{R}_1^{\mathrm{SF}}(k) = \sum_{i\bar{a}} r_i^a(k) \hat{\bar{a}}^\dagger \hat{i}$$
$$\hat{R}_2^{\mathrm{SF}}(k) = \frac{1}{2} \sum_{ij\bar{a}b} r_{ij}^{ab}(k) \hat{\bar{a}}^\dagger \hat{i} \hat{\bar{b}}^\dagger \hat{j} + \frac{1}{2} \sum_{i\bar{j}\bar{a}\bar{b}} r_{ij}^{ab}(k) \hat{\bar{a}}^\dagger \hat{i} \hat{\bar{b}}^\dagger \hat{\bar{j}}$$

Thus, $\hat{R}^{\mathrm{SF}}(k)$ reduces the M_s value by one with respect to the high-spin reference state to target low-spin states,

$$\hat{R}_{M_s=-1}^{\mathrm{SF}}(k) = \hat{R}_1^{\mathrm{SF}}(k) + \hat{R}_2^{\mathrm{SF}}(k) + \ldots$$

To arrive at the EOM-CC working equations, we employ the normal-product form of the Hamiltonian, $\hat{H}_N = \hat{H} - \langle \Phi_0 | \hat{H} | \Phi_0 \rangle$. The Schrödinger equation for the ground state ($k = 0$) then reads

$$\hat{H}_N \left| \Psi_0 \right\rangle = \Delta E_0 \left| \Psi_0 \right\rangle , \tag{3}$$

where ΔE_0 is the correlation energy with respect to the CC reference determinant $|\Phi_0\rangle$. The excited (or ionized, etc.) states are obtained from solving the corresponding EOM equations

$$\begin{aligned} \hat{H}_N \hat{R}(k) \left| \Psi_0 \right\rangle &= \Delta E_k \hat{R}(k) \left| \Psi_0 \right\rangle \\ \hat{H}_N \hat{R}(k) e^{\hat{T}} \left| \Phi_0 \right\rangle &= \Delta E_k \hat{R}(k) e^{\hat{T}} \left| \Phi_0 \right\rangle , \end{aligned} \tag{4}$$

where ΔE_k is the energy difference with respect to the Fermi vacuum expectation value $|\Phi_0\rangle$. Subtracting the CC equations for the ground state from eq. (4), we obtain the well-known EOM equations for the $\hat{R}$ amplitudes,

$$[\hat{H}_N, \hat{R}] \left| \Psi_0 \right\rangle = \omega \hat{R} \left| \Psi_0 \right\rangle , \tag{5}$$

where $\omega = \Delta E - \Delta E_0$ is the change in energy associated with the, for instance, excitation or (single, double, etc.) ionization process with respect to the CC ground state. The total electronic energies of the targeted (ionized, etc.) states are then deduced from the total energy of the CC reference function E_0 and the excitation (or ionization, etc.) energy, $E_k = E_0 + \omega$. Since $\hat{R}$ and $\hat{T}$ commute, eq. (5) can be simplified as

$$\begin{aligned} e^{-\hat{T}} \hat{H}_N e^{\hat{T}} \hat{R}(k) \left| \Phi_0 \right\rangle &= \omega \hat{R}(k) \left| \Phi_0 \right\rangle \\ \hat{\mathcal{H}}_N \hat{R}(k) \left| \Phi_0 \right\rangle &= \omega \hat{R}(k) \left| \Phi_0 \right\rangle , \end{aligned} \tag{6}$$

where we introduced the similarity transformed Hamiltonian of CC theory in its normal-product form $\hat{\mathcal{H}}_N = e^{-\hat{T}} \hat{H}_N e^{\hat{T}}$. The excitation, ionization, etc. energies are thus the eigenvalues of a non-Hermitian matrix, which can be iteratively diagonalized using, for instance, non-Hermitian extensions of the Davidson algorithm to determine the lowest-lying states.

The $S_z = -\frac{1}{2}$ IP-EOM manifold

The diagonalization of the matrix representation of the similarity-transformed Hamiltonian $\hat{\mathcal{H}}_N$ of the $S_z = -\frac{1}{2}$ IP-EOM model can be performed in a specific configurational subspace spanned by the Slater determinants $|\Phi_i\rangle, \left|\Phi_{ij}^{\ a}\right\rangle, \left|\Phi_{i\bar{j}}^{\ \bar{a}}\right\rangle$ containing $N-1$ electrons,

$$\begin{bmatrix} \langle\Phi_i|\,\hat{\mathcal{H}}_N\,|\Phi_k\rangle & \langle\Phi_i|\,\hat{\mathcal{H}}_N\,\left|\Phi_{kl}^{\ b}\right\rangle & \langle\Phi_i|\,\hat{\mathcal{H}}_N\,\left|\Phi_{k\bar{l}}^{\ \bar{b}}\right\rangle \\ \left\langle\Phi_{ij}^{\ a}\right|\hat{\mathcal{H}}_N\,|\Phi_k\rangle & \left\langle\Phi_{ij}^{\ a}\right|\hat{\mathcal{H}}_N\,\left|\Phi_{kl}^{\ b}\right\rangle & \left\langle\Phi_{ij}^{\ a}\right|\hat{\mathcal{H}}_N\,\left|\Phi_{k\bar{l}}^{\ \bar{b}}\right\rangle \\ \left\langle\Phi_{i\bar{j}}^{\ \bar{a}}\right|\hat{\mathcal{H}}_N\,|\Phi_k\rangle & \left\langle\Phi_{i\bar{j}}^{\ \bar{a}}\right|\hat{\mathcal{H}}_N\,\left|\Phi_{kl}^{\ b}\right\rangle & \left\langle\Phi_{i\bar{j}}^{\ \bar{a}}\right|\hat{\mathcal{H}}_N\,\left|\Phi_{k\bar{l}}^{\ \bar{b}}\right\rangle \end{bmatrix}. \tag{7}$$

The $\hat{R}^{S_z=-\frac{1}{2}}$ excitation operator generates a projection manifold that contains, for example, the following open-shell configurations

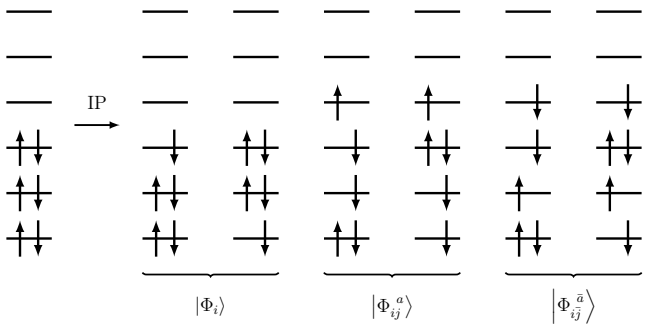

The $S_z = -\frac{3}{2}$ IP-EOM manifold

The diagonalization of the matrix representation of the similarity-transformed Hamiltonian $\hat{\mathcal{H}}_N$ of the $S_z = -\frac{3}{2}$ IP-EOM model can be performed in a specific configurational subspace spanned by the Slater determinants $\left|\Phi_{ij}^{\ \bar{a}}\right\rangle$ containing $N-1$ electrons,

$$\left[\left\langle\Phi_{ij}^{\ \bar{a}}\right|\hat{\mathcal{H}}_N\,|\Phi_{lm}^{\ \bar{c}}\rangle\right]. \tag{8}$$

The $\hat{R}^{S_z=-\frac{3}{2}}$ excitation operator generates a projection manifold that contains, for example, the following open-shell configurations

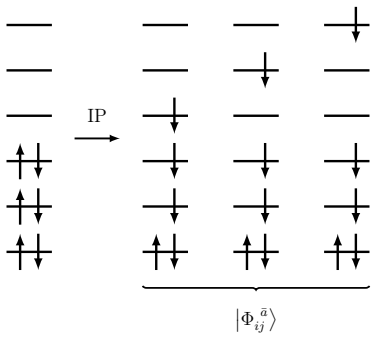

The $S_z = -1$ DIP-EOM manifold

The diagonalization of the matrix representation of the similarity-transformed Hamiltonian $\hat{\mathcal{H}}_N$ of the $S_z = -1$ DIP-EOM model can be performed in a specific configurational subspace spanned by the Slater determinants spanned by $|\Phi_{ij}\rangle$, $\left|\Phi_{ijk}^{\ a}\right\rangle$, $\left|\Phi_{ij\bar{k}}^{\ \bar{a}}\right\rangle$ for $N-2$ electrons,

$$\begin{bmatrix} \langle\Phi_{ij}|\,\hat{\mathcal{H}}_N\,|\Phi_{lm}\rangle & \langle\Phi_{ij}|\,\hat{\mathcal{H}}_N\,|\Phi_{lmn}^{\ \ c}\rangle & \langle\Phi_{ij}|\,\hat{\mathcal{H}}_N\,|\Phi_{lm\bar{n}}^{\ \ \bar{c}}\rangle \\ \left\langle\Phi_{ijk}^{\ a}\right|\hat{\mathcal{H}}_N\,|\Phi_{lm}\rangle & \left\langle\Phi_{ijk}^{\ a}\right|\hat{\mathcal{H}}_N\,|\Phi_{lmn}^{\ \ c}\rangle & \left\langle\Phi_{ijk}^{\ a}\right|\hat{\mathcal{H}}_N\,|\Phi_{lm\bar{n}}^{\ \ \bar{c}}\rangle \\ \left\langle\Phi_{ij\bar{k}}^{\ \bar{a}}\right|\hat{\mathcal{H}}_N\,|\Phi_{lm}\rangle & \left\langle\Phi_{ij\bar{k}}^{\ \bar{a}}\right|\hat{\mathcal{H}}_N\,|\Phi_{lmn}^{\ \ c}\rangle & \left\langle\Phi_{ij\bar{k}}^{\ \bar{a}}\right|\hat{\mathcal{H}}_N\,|\Phi_{lm\bar{n}}^{\ \ \bar{c}}\rangle \end{bmatrix}. \tag{9}$$

The $\hat{R}^{S_z=-1}$ excitation operator generates a projection manifold that contains, for example, the following open-shell configurations

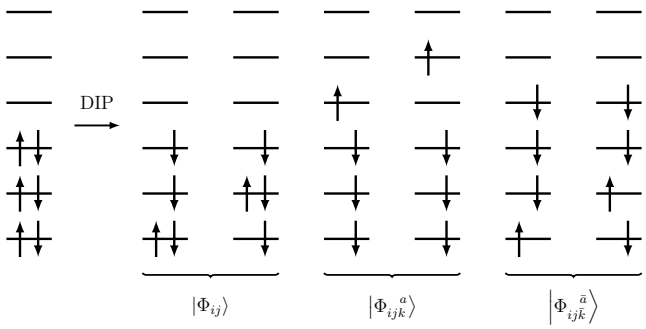

The $S_z = -2$ DIP-EOM manifold

The diagonalization of the matrix representation of the similarity-transformed Hamiltonian $\hat{\mathcal{H}}_N$ of the $S_z = -2$ DIP-EOM model can be performed in a specific configurational subspace spanned by the Slater determinants $\left|\Phi_{ijk}^{\ \bar{a}}\right\rangle$ containing $N-2$ electrons,

$$\left[\left\langle\Phi_{ijk}^{\ \bar{a}}\right|\hat{\mathcal{H}}_N\,|\Phi_{lmn}^{\ \ \bar{c}}\rangle\right]. \tag{10}$$

The $\hat{R}^{S_z=-2}$ excitation operator generates a projection manifold that contains, for example, the following open-shell configurations

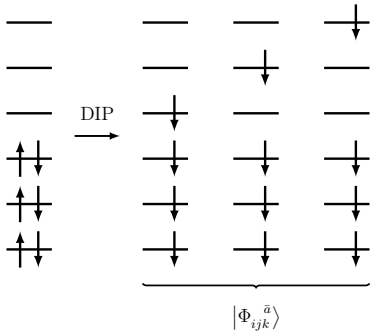

The $S_z = 0$ DIP-EOM manifold

The diagonalization of the matrix representation of the similarity-transformed Hamiltonian $\hat{\mathcal{H}}_N$ of the $S_z = 0$ DIP-EOM model can be performed in a specific configurational subspace spanned by the Slater determinants spanned by $\left|\Phi_{i\bar{j}}\right\rangle, \left|\Phi_{i\bar{j}k}^{\ a}\right\rangle, \left|\Phi_{i\bar{j}\bar{k}}^{\ \bar{a}}\right\rangle$ for $N-2$ electrons,

$$\begin{bmatrix} \left\langle \Phi_{i\bar{j}} \right| \hat{\mathcal{H}}_N \left| \Phi_{l\bar{m}} \right\rangle & \left\langle \Phi_{i\bar{j}} \right| \hat{\mathcal{H}}_N \left| \Phi_{l\bar{m}n}^{\ \ c} \right\rangle & \left\langle \Phi_{i\bar{j}} \right| \hat{\mathcal{H}}_N \left| \Phi_{l\bar{m}\bar{n}}^{\ \ \bar{c}} \right\rangle \\ \left\langle \Phi_{i\bar{j}k}^{\ a} \right| \hat{\mathcal{H}}_N \left| \Phi_{l\bar{m}} \right\rangle & \left\langle \Phi_{i\bar{j}k}^{\ a} \right| \hat{\mathcal{H}}_N \left| \Phi_{l\bar{m}n}^{\ \ c} \right\rangle & \left\langle \Phi_{i\bar{j}k}^{\ a} \right| \hat{\mathcal{H}}_N \left| \Phi_{l\bar{m}\bar{n}}^{\ \ \bar{c}} \right\rangle \\ \left\langle \Phi_{i\bar{j}\bar{k}}^{\ \bar{a}} \right| \hat{\mathcal{H}}_N \left| \Phi_{l\bar{m}} \right\rangle & \left\langle \Phi_{i\bar{j}\bar{k}}^{\ \bar{a}} \right| \hat{\mathcal{H}}_N \left| \Phi_{l\bar{m}n}^{\ \ c} \right\rangle & \left\langle \Phi_{i\bar{j}\bar{k}}^{\ \bar{a}} \right| \hat{\mathcal{H}}_N \left| \Phi_{l\bar{m}\bar{n}}^{\ \ \bar{c}} \right\rangle \end{bmatrix}. \tag{11}$$

The $\hat{R}^{S_z=0}$ excitation operator generates a projection manifold that contains, for example, the following open-shell configurations

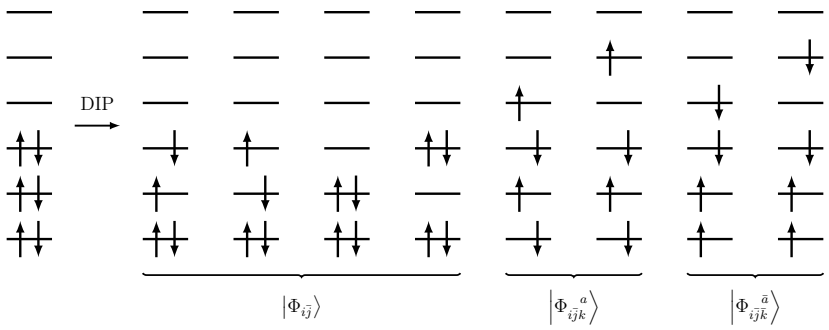

Note that only the S_z value is constrained in each IP-EOM model. Thus, $\hat{R}^{S_z=0}$ can be used to describe singlet and triplet states, $\hat{R}^{S_z=-\frac{1}{2}}$ doublet and quartet states, $\hat{R}^{S_z=-1}$ triplet and quintet states. By construction, $\hat{R}^{S_z=-\frac{3}{2}}$ and $\hat{R}^{S_z=-2}$ can only describe quartet and quintet states, respectively.

S2 Computational Details

All pCCD, IP-EOM-pCCD, and DIP-EOM-pCCD calculations were performed in a developer version of the PyBEST software package.[1–3] For a direct comparison to reference data, we used Dunning's cc-pVTZ[4] (CH_2, NH_2^+, SiH_2, PH_2^+, benzyne isomers), cc-pVQZ[5] (CH_2), and aug-cc-pVDZ[6] (N-N'-dimethylpiperazine; DMP^+) basis sets for all atoms. Furthermore, a frozen core was applied in all pCCD and (D)IP-EOM calculations, where only the valence electrons were considered in the correlation calculations. In all pCCD calculations, the orbitals were allowed to relax freely within C_1 point group symmetry.

For all open-shell molecules, we performed variational orbital-optimized pCCD calculations for closed-shell species that were obtained by adding one (two) electron(s) to the molecules in question. Specifically for DMP^+, we optimized pCCD for the corresponding closed-shell uncharged species DMP. For all singlet-triplet gaps, the pCCD reference wave function was obtained by adding two electrons in orbital-optimized pCCD calculations.

For CH_2, we estimated the complete basis set (CBS) limit values for the adiabatic energy differences of the four energetically lowest-lying states for $S_z = 0, -1$. For that purpose, we applied a two-point procedure, where the asymptotic value of the total electronic energies in the CBS limit is

extrapolated using the following fitting function

$$E_{\mathrm{CBS}} = E_X + aX^{-3}. \tag{12}$$

In the above equation, X is the cardinal number of the atomic basis set ($X = 3$ for the cc-pVTZ basis, $X = 4$ for the cc-pVQZ basis, etc.), E_X is the corresponding total energy of a specific state, and a is some fitting parameter. In this work, we approximated the CBS limit for $X = 3, 4$.

The molecular geometries were taken from refs. 7,8 (CH_2), 8,9 (NH_2^+), 8,10 (SiH_2), 8,11 (PH_2^+), 8 (*o*-, *m*-, and *p*-benzyne), and 12–14 (DMP^+).

S3 PES of DMP^+

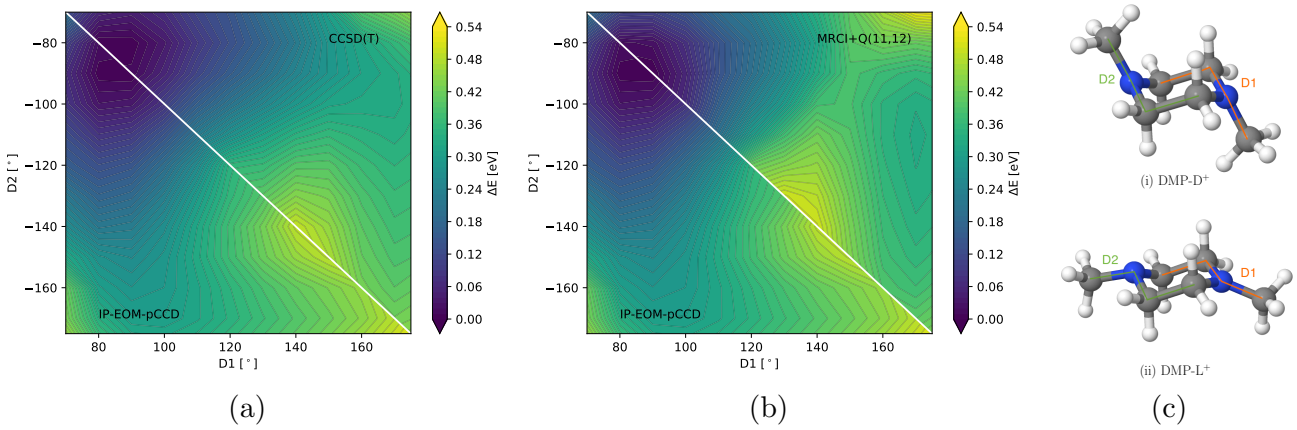

(a) (b) (c)

Figure S1: PESs for (a) IP-EOM-pCCD/aug-cc-pVDZ (bottom) and CCSD(T)/aug-cc-pVDZ[12,13] (top) and (b) IP-EOM-pCCD/aug-cc-pVDZ (bottom) and MRCI+Q(11,12)/cc-pVDZ[12,13] (top) scanned for different dihedral angels D1 and D2 as indicated in (c). For all surfaces, the structures fom refs. 12–14 are used. (c) The relaxed structures of the delocalized ($DMP\text{-}D^+$) and localized ($DMP\text{-}L^+$) state of DMP^+ including both dihedral angles.

S4 Methylene and its isovalent series

S4.1 The electronic structure of CH_2, NH_2^+, SiH_2, and PH_2

The ground state of CH_2 and NH_2^+ is a triplet state $^3B_1$ with a dominant electronic configuration $(1a_1)^2(2a_1)^2(1b_2)^2(1b_1)(3a_1)$. The lowest-lying excited state is a closed-shell singlet state $^1A_1$ with two main electronic configurations, $(1a_1)^2(2a_1)^2(1b_2)^2(3a_1)^2$ and $(1a_1)^2(2a_1)^2(1b_2)^2(1b_1)^2$. The second lowest-lying excited state is an open-shell singlet state $^1B_1$, whose electronic structure features a similar leading electronic configuration as the triplet ground state, namely $(1a_1)^2(2a_1)^2(1b_2)^2(1b_1)(3a_1)$. Similar to the first $^1A_1$ state, the third excited state is a closed-shell singlet, whose leading electronic configuration is characterized as $(1a_1)^2(2a_1)^2(1b_2)^2(1b_1)^2$ followed by the $(1a_1)^2(2a_1)^2(1b_2)^2(3a_1)^2$ configuration. Thus, the electronic structures of the four lowest-lying states differ in their occupation

of the two valence molecular orbitals $1b_1$ and $3a_1$, respectively. While the former ($1b_1$) represents an sp^2-hybridized orbital, the former ($3a_1$) is derived from a p-orbital of the heavy atom center.

In contrast to the CH_2 and NH_2^+ molecules, the isovalent SiH_2 and PH_2 species have a closed-shell singlet ground state $^1A_1$, where the valence part of the electronic configuration has two main electronic configurations, $(4a_1)^2(2b_2)^2(5a_1)^2$ followed by $(4a_1)^2(2b_2)^2(2b_1)^2$. The first excited state is an open-shell triplet state $^3B_1$, whose dominant electronic configuration features a singly-occupied $5a_1$ and $2b_1$ orbital, that is, $(4a_1)^2(2b_2)^2(5a_1)(2b_1)$. Similar to CH_2 and NH_2^+, the next excited state is an open-shell singlet $^1B_1$ state, followed by a closed-shell singlet state $^1A_1$. The $^1B_1$ excited state has a similar dominant electronic configuration as the lowest-lying triplet state, where the $5a_1$ and $2b_1$ valence orbitals are singly occupied. In the fourth excited state ($^1A_1$), the main electronic configurations have doubly-occupied $2b_1$ or $5a_1$ orbitals, which results in $(4a_1)^2(2b_2)^2(2b_1)^2$ and $(4a_1)^2(2b_2)^2(5a_1)^2$.

S4.2 CBS results for methylene

Table S1 collects the extrapolated excitation energies to the basis set limit for the CH_2 molecule. DIP-EOM-pCCD underestimates the lowest-lying singlet-triplet gap by approximately 0.2 eV, while the energy difference between the $^3B_1$ and $^1B_1$ states decreases to 1.547 eV and differs by about 0.12 eV from the experimental reference value. Again, the performance of DIP-EOM-pCCD is comparable, albeit slightly better than the more expensive DIP-EOM-CCSD approach.

Table S1: Extrapolated total energies (E_h) for the ground state of CH_2 and extrapolated excitation energies (eV) for the three lowest-lying excited states obtained by different electronic structure methods.

CH_2	$^3B_1$	$^1A_1$	$^1B_1$	2^1A_1
DIP-EOM-pCCD	−39.03537	0.205	1.547	2.598
DIP-EOM-CCSD [22]	–	0.178	–	–
DEA-EOM-CCSD [22]	–	0.388	–	–
CCSD(T) [22]	–	0.399	–	–
Experiment [23]		0.390	1.425	

S5 Total and relative energies for benzyne isomers

The ground state of the benzyne isomers is a closed-shell singlet, while the lowest-lying excited state is a triplet state. With increasing diradical character, this singlet-triplet gap reduces in the sequence ortho→meta→para.

Table S2: Total energies [E_h] for the ground state and the adiabatic excitation energy [eV] to the lowest-lying triplet state of ortho-, meta, and para-benzyne.

	o-benzyne		*m*-benzyne		*p*-benzyne	
	$^1A_1$	$^3B_2$	$^1A_1$	$^3B_2$	^1A_g	$^3B_{1u}$
DIP-EOM-pCCD	−229.85076	1.398	−229.83641	0.856	−229.81474	0.221
DIP-EOM-CCSD [22]	–	1.847	–	0.854	–	0.191
DEA-EOM-CCSD [22]	–	1.565	–	0.794	–	0.147
SF-CIS [8]	−229.49504	1.007	−229.47187	0.166	−229.46472	0.014
SF-CIS(D) [8]	−230.45684	1.548	−230.38757	0.842	−230.41234	0.092
SF-OD [8]	−230.50269	1.632	−230.47817	0.837	−230.45743	0.171
CCSD [22]	–	1.327	–	0.455	–	−0.833
CCSD(T) [22]	–	1.604	–	0.958	–	0.156
Experiment [24]		1.628±0.013		0.911±0.014		0.165±0.016

References

[1] F. Brzęk, A. Leszczyk, A. Nowak, K. Boguslawski, D. Kędziera, P. Tecmer and P. S. Żuchowski, *Pythonic Black-box Electronic Structure Tool (PyBEST v1.1.0)*, 2021, 10.5281/zenodo.5055156.

[2] 2021, See `http://pybest.fizyka.umk.pl` for more information about PyBEST (accessed July 1, 2021).

[3] K. Boguslawski, A. Leszczyk, A. Nowak, F. Brzęk, P. S. Żuchowski, D. Kędziera and P. Tecmer, *Comput. Phys. Commun.*, 2021, **264**, 107933.

[4] R. A. Kendall, T. H. Dunning Jr., and R. J. Harrison, *J. Chem. Phys.*, 1992, **96**, 6796–6806.

[5] D. E. Woon and T. H. Dunning Jr., *J. Chem. Phys.*, 1993, **98**, 1358–1371.

[6] R. A. Kendall, T. H. Dunning and R. J. Harrison, *J. Chem. Phys.*, 1992, **96**, 6796–6806.

[7] C. D. Sherrill, M. L. Leininger, T. J. Van Huis and H. F. Schaefer III, *J. Chem. Phys.*, 1998, **108**, 1040–1049.

[8] L. V. Slipchenko and A. I. Krylov, *J. Chem. Phys.*, 2002, **117**, 4694.

[9] J. C. Stephens, Y. Yamaguchi, C. D. Sherrill and H. F. Schaefer III, *J. Phys. Chem. A*, 1998, **102**, 3999–4006.

[10] Y. Yamaguchi, T. J. Van Huis, C. D. Sherrill and H. F. Schaefer III, *Theor. Chem. Acc.*, 1997, **97**, 341–349.

[11] T. J. Van Huis, Y. Yamaguchi, C. D. Sherrill and H. F. Schaefer, *J. Phys. Chem. A*, 1997, **101**, 6955–6963.

[12] M. Gałyńska, V. Ásgeirsson, H. Jónsson and R. Björnsson, 2020, arXiv:2007.06125 [physics.chem-ph].

[13] M. Gałyńska, V. Ásgeirsson, H. Jónsson and R. Björnsson, *J. Phys. Chem. Lett.*, 2021, **12**, 1250–1255.

[14] The molecular structures of the DMP^+ molecule were provided by Marta Gałyńska.

[15] J. F. Stanton and R. J. Bartlett, *J. Chem. Phys.*, 1993, **98**, 7029–7039.

[16] J. Jankowski, K. Kowalski and P. Jankowski, *Chem. Phys. Lett.*, 1994, **222**, 608–614.

[17] R. J. Bartlett and M. Musiał, *Rev. Mod. Phys.*, 2007, **79**, 291–350.

[18] A. I. Krylov, *Ann. Rev. Phys. Chem.*, 2008, **59**, 433–462.

[19] K. Sneskov and O. Christiansen, *WIREs Comput. Mol. Sci.*, 2012, 566–584.

[20] R. J. Bartlett, *WIREs Comput. Mol. Sci.*, 2012, **2**, 126–138.

[21] D. Casanova and A. I. Krylov, *Phys. Chem. Chem. Phys.*, 2020, **22**, 4326–4342.

[22] A. Perera, R. W. Molt Jr., V. F. Lotrich and R. J. Bartlett, *Theor. Chem. Acc.*, 2014, **133**, 1514.

[23] P. Jensen and P. R. Bunker, *J. Chem. Phys.*, 1988, **89**, 1327–1332.

[24] P. G. Wenthold, R. R. Squires and W. C. Lineberger, *J. Am. Chem. Soc.*, 1998, **120**, 5279–5290.